

Analytical Methods

Accepted Manuscript

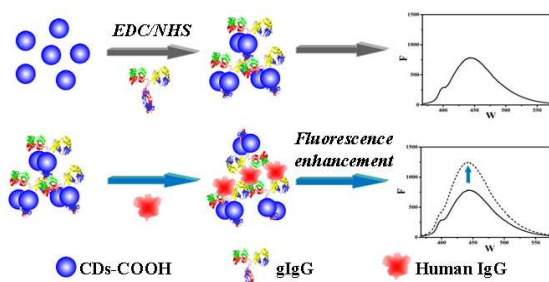


This is an *Accepted Manuscript*, which has been through the Royal Society of Chemistry peer review process and has been accepted for publication.

Accepted Manuscripts are published online shortly after acceptance, before technical editing, formatting and proof reading. Using this free service, authors can make their results available to the community, in citable form, before we publish the edited article. We will replace this *Accepted Manuscript* with the edited and formatted *Advance Article* as soon as it is available.

You can find more information about *Accepted Manuscripts* in the [Information for Authors](#).

Please note that technical editing may introduce minor changes to the text and/or graphics, which may alter content. The journal's standard [Terms & Conditions](#) and the [Ethical guidelines](#) still apply. In no event shall the Royal Society of Chemistry be held responsible for any errors or omissions in this *Accepted Manuscript* or any consequences arising from the use of any information it contains.



A novel fluorescence immunoassay protocol, using high quantum yield of carbon dots as fluorescent labels, was developed for rapid quantitative determination of the model analyte human immunoglobulin G.

Fluorescence immunoassay based on carbon dots as labels for the detection of human immunoglobulin G

Lei Zhu, Xin Cui, Jing Wu, Zhenni Wang, Peiyao Wang, Yu Hou and Mei Yang*

School of Chemistry and Chemical Engineering,

Liaoning Normal University, Dalian 116029, P. R. China

E-mail: yangmeils@163.com

Telephone: +86-411-82156606

ABSTRACT

A rapid, selective and environmentally friendly fluorescence immunoassay strategy based on carbon dots (CDs) is developed for the detection of human immunoglobulin G (IgG, antigen). Firstly, in this protocol, CDs with high quantum yield were synthesized by hydrothermal process using citric acid as a carbon source and then carboxylated by bath sonication with NaOH and ClCH₂COONa. Subsequently, carboxyl-functionalized CDs were conjugated with goat antihuman IgG (gIgG, antibody) using an EDC/NHS amidization method to obtain the CDs-labeled gIgG, and this obtained conjugate CDs-gIgG was then incubated with a limited amount of human IgG for immunoreaction between antigen and antibody. The immunocomplex formed on the surface of carboxylated CDs resulted in the increase of fluorescence intensity. Under the optimal conditions, a linear relationship between fluorescence change ratio $(F-F_0)/F_0$ and human IgG concentration in a range from 0.05 to 2.0 $\mu\text{g mL}^{-1}$ was obtained with a detection limit of 0.01 $\mu\text{g mL}^{-1}$. This method has been successfully applied to the determination of IgG in human serum, with recoveries in the range of 95.8%-111.5%. The results indicate the great promise for CDs as labels in fluorescence immunoassays.

Keywords: Carbon dots; Human IgG; Fluorescence immunoassay

1. Introduction

In recent years, fluorescence immunoassays based on selective antigen-antibody binding and fluorescent labels have gained increasing importance^{1,2} in clinical diagnoses, environment, and biochemical studies.^{3,4} The conventional fluorescent labels used in fluorescence immunoassay biological detections are organic dyes.^{5,6} The major advantages of organic dyes are their small size, good biocompatibility and relatively high fluorescent intensity. However, they are easily photobleached⁷ and often have narrow absorption and broad emission spectra with long tailing, resulting in lower detection sensitivity.⁸ Hence, much attention has been paid to semiconductor quantum dots (QDs) such as CdSe and CdTe due to their bright photoluminescence, high quantum yields, relatively good photostability, large Stokes shift, narrow emission, and broad excitation.⁹ Unfortunately, the application of QDs in biological field is limited since it exhibits aggregation, difficult delivery and cumulative toxicity in live cells.¹⁰ Therefore, selecting an environmentally friendly material with excellent photoluminescent property as fluorescent label for the sensitive and selective antigen or antibody detection is in ever-increasing demand.

The recently emerged carbon nanomaterials, carbon dots (CDs), are found to be promising replacements for the traditional heavy-metal-based QDs and organic dyes. CDs are quasispherical nanoparticles (<10 nm) with good water solubility, easy functionalization, high resistance to photobleaching, low toxicity and excellent biocompatibility,¹¹ for which a variety of simple, fast and cheap synthetic routes are available.¹²⁻¹⁶ The above advantages allow one to use CDs as fluorescent labels for bioimaging and biological sensing.¹⁷⁻²² Until now, based on the variations of fluorescence intensity, such CDs labels have been used to detect many substances such as Ca²⁺,¹⁷ DNA¹⁸ and thrombin.¹⁹ Nevertheless, to our knowledge, few researches have been reported to employ CDs as fluorescent labels for detecting antigen or antibody.

By taking the advantages of CDs, a fluorescence immunoassay platform using CDs as labels was designed. Herein, we choose human immunoglobulin G (IgG) as the model analyte. Specifically, CDs with high quantum yield were synthesized and

1
2
3
4 carboxylated, and then carboxyl-functionalized CDs were further used to label the
5
6 goat anti-human IgG (gIgG) to obtain the CDs-gIgG conjugate. In the sensing process,
7
8 the addition of human IgG would bind the gIgG due to the specific antigen-antibody
9
10 interaction, which gave rise to the enhancement of fluorescence intensity. Furthermore,
11
12 quantitative measurements of IgG in human sera have been demonstrated, which
13
14 provide a promising potential in clinical diagnosis.

17 18 **2. Experimental**

19 20 **2.1. Materials and measurements**

21
22 Human immunoglobulin G (IgG) and goat anti-human immunoglobulin G (gIgG)
23
24 were all purchased from Beijing Biocity technology Co., Ltd (China). Bovine serum
25
26 albumin (BSA) was provided by Amresco Inc. (USA). Sodium chloroacetate
27
28 (ClCH₂COONa), 1-ethyl-3-(3-dimethylaminopropyl) carbodiimide hydrochloride
29
30 (EDC) and N-Hydroxysuccinimide (NHS) were obtained from GL Biochem Ltd.
31
32 (Shanghai, China). Dialysis bags (MW 3500, MW 8000-14000) were supplied by
33
34 Union Carbide Co. (USA). The serum samples were provided by seven healthy adult
35
36 volunteers. The detection buffer was phosphate buffered saline (PBS, 0.1 M). All
37
38 other chemicals were of analytical grade and used without further purification, and
39
40 doubly distilled water was used throughout the experiment.

41
42 The UV-Vis absorption spectra and the fluorescence spectra were obtained using
43
44 a UV-240 UV-Vis spectrophotometer (Shimadzu Co., Japan) and a F-7000
45
46 fluorescence spectrophotometer (Hitachi Ltd, Japan), respectively. Fourier transform
47
48 infrared spectra (FT-IR) in the 4000 to 400cm⁻¹ region were recorded on a Tensor-27
49
50 FT-IR spectroscope (Bruker Instrument Co., Germany).

51 52 53 **2.2. Preparation of CDs and carboxyl-functionalized CDs (CDs-COOH)**

54
55 CDs were prepared according to a reported method.¹⁵ In detail, citric acid (3.0 g)
56
57 and ethylenediamine (1875 μL) were dissolved in doubly distilled water (30 mL).
58
59 Then the solution was transferred to a 50 mL Teflon-lined stainless steel autoclave
60
and heated at 150 °C for 5 h. After the reaction, the reactors were cooled to room

1
2
3
4 temperature. The product, which was brown-black and transparent, was subjected to
5
6 dialysis against doubly distilled water in order to obtain the CDs.

7
8 A simple method was used to introduce carboxyl groups.²³ Briefly, 50.0 mg of
9
10 as-prepared CDs were dispersed in 50 mL of aqueous solution containing 2.5 g of
11
12 NaOH and 2.5 g of ClCH₂COONa, followed by bath sonication for 3 h. After these
13
14 treatments, the resulting CDs-COONa were neutralized with HCl to obtain
15
16 CDs-COOH. Finally, the CDs-COOH suspension was dialyzed against doubly
17
18 distilled water for over 2 days to remove all ions.

21 22 **2.3. Preparation of the CDs-gIgG conjugate**

23
24 According to the reported procedure,²⁴ 1.5 mg of CDs-COOH were mixed with
25
26 EDC at 400 mM and NHS at 100 mM in 1.5 mL of 0.1 M PBS buffer (pH 7.4) and
27
28 incubated at 37 °C for 30 min with magnetic stirring at 10 rpm. Then 2.0 mL of 30 μg
29
30 mL⁻¹ gIgG solution was added to the reaction mixture and further incubated at 37 °C
31
32 for 2 h. Finally, the solution was kept at 4 °C overnight to deactivate the remaining
33
34 EDC-NHS. The conjugate solution was dialyzed for 2 days to remove the free
35
36 non-conjugated CDs-COOH, when the dialysate had hardly any UV-Vis absorption
37
38 values and fluorescence signals.

39 40 41 42 **2.4. Determination of quantum yield**

43
44 The quantum yield (Φ) of CDs and the conjugate were measured by comparing
45
46 the integrated photoluminescence intensities and the absorbency values with those of
47
48 the reference quinine sulfate (QS). The quinine sulfate (literature Φ=0.54 at 360 nm)
49
50 was dissolved in 0.1 M H₂SO₄ (refractive index (η) of 1.33) and the CDs were
51
52 dissolved in doubly distilled water (η=1.33), as reported by Yang et al.²⁵

$$53
54
55 \Phi = \Phi_R \times \frac{I}{I_R} \times \frac{A_R}{A} \times \frac{\eta^2}{\eta_R^2}$$

56
57
58 Where Φ is the quantum yield, I is the measured integrated emission intensity, η
59
60 is the refractive index, and A is the optical density, respectively. The subscript R refers
to the reference fluorophore of known quantum yield.

2.5. Pretreatment of human serum samples

Human blood samples were provided by seven healthy adult volunteers. These samples were centrifuged at 2000 rpm for 15 min to obtain serum, and were stored at -20 °C until analysis, and diluted 2.5×10^4 fold with PBS (pH 7.4) before analysis.

2.6. Fluorescence immunoassay for determination of human IgG

In a typical experiment, different volumes of human IgG and 30 μL of 0.5 mg mL^{-1} CDs-gIgG were added to 0.1 M PBS buffer solution (pH 7.4) with a final volume of 1 mL, and the resulting mixture was incubated at 37 °C for 30 min to obtain the CDs-gIgG-human IgG immunocomplex. The fluorescence emission spectra of the immunocomplex were measured with an excitation wavelength of 347 nm in the fluorescence spectrophotometer. The ratio of fluorescence change $(F-F_0)/F_0$ was used for quantification of human IgG, which F_0 was the blank fluorescence intensity without human IgG.

3. Results and discussion

3.1. Investigation of the spectral properties of CDs and CDs-gIgG conjugate

The CDs were synthesized from citric acid and ethylenediamine through a simple, convenient and one-step hydrothermal method.¹⁵ As shown in Fig. 1A, the fluorescent emission peak of CDs (A) shifted to a longer wavelength with increasing excitation wavelength. This behavior of excitation-dependent reflected not only the effects from different sizes but also a considerable distribution of emissive trap sites on each carbon dot. Interestingly, in a control experiment, the emission peak of CDs (B) at various excitation wavelengths did not shift, and the maximum emission wavelength remained at 440 nm, which is shown clearly in Fig. 1B. The property of excitation-independent behavior could be explained by the uniform size and emissive sites. The quantum yield of CDs (A) was obtained with the value of 6.7% when the ethylenediamine was omitted, as shown in Table 1, in the presence of ethylenediamine, the quantum yield of CDs (B) rose to 74.6% dramatically, which was almost equal to

those of fluorescent dyes. Thus, we select CDs (B) as an environmentally friendly fluorescence immune probe to label the gIgG for synthesis of the CDs-gIgG conjugate.

A UV-Vis absorption measurement was performed to investigate the formation of the CDs-gIgG conjugate. As shown in Fig. 1C, the absorption peaks were located at 344 nm for the aqueous solutions of CDs-COOH and CDs-gIgG. Moreover, the conjugate showed strong absorption at about 270 nm, indicating the gIgG antibody has been labeled onto the CDs-COOH. Their bright blue color was strong enough to be observed under UV light illumination by naked eyes (Fig. 1C, inset).

As shown in Fig. 1D, CDs-COOH and CDs-gIgG displayed similar excitation and emission spectra. When being excited at 347 nm, both CDs-COOH and CDs-gIgG exhibited the strongest emission band centered at 445 nm. The change in intensity was due to the different concentrations of CDs in CDs-COOH and the conjugate. As shown in Table 1, the quantum yield of CDs-COOH decreased greatly than CDs, which was attributed to the increase of electron-withdrawing carboxyl group. Moreover, the quantum yield of the conjugate was calculated to be 7.3%, and is nearly equal to the one of CDs-COOH (7.2%), reflecting that the conjugation hardly altered the inherent emission features of the CDs-COOH.

Fluorescence polarization (FP) measurements are based on the assessment of molecular rotations of fluorescent molecules excited by polarized light.²⁶ The fluorescent substance with low molecular weight can rotate rapidly and results in low P values. When fluorescent substance is bound to a very large protein such as antibody, a higher P values are obtained. FP is defined as:

$$P = \frac{I_{//} - G \times I_{\perp}}{I_{//} + G \times I_{\perp}} \quad (G = \frac{i_{\perp}}{i_{//}})$$

where $I_{//}$, $i_{//}$ and I_{\perp} , i_{\perp} represent the horizontally and vertically polarized emission intensities, respectively, and G is a correction factor which detects the instrumental sensitivity of the polarization direction of emission.

Based on the above principle, the fluorescence emission intensities of the CDs-COOH and CDs-gIgG were measured under 347 nm excitation and 445 nm

1
2
3
4 emission by selecting photometry as the fluorescence measurement type, and the
5
6 corresponding polarization values were calculated according to the FP equation. The
7
8 binding could be monitored simply by comparing the polarization values of
9
10 CDs-COOH and CDs-gIgG. Polarization value is a ratio, and does not change with
11
12 fluorescence intensity, therefore, different concentrations of samples should have the
13
14 same value. As shown in Table 2, the FP values were much higher after the
15
16 CDs-COOH was bounded to the gIgG antibody.

17
18 To further demonstrate the successful labeling of gIgG with CDs-COOH, the
19
20 as-prepared CDs, CDs-COOH and CDs-gIgG are analyzed by FT-IR spectroscopy,
21
22 respectively (Fig. 2). In the FT-IR spectrum of CDs, stretching vibrations of C-OH
23
24 and asymmetric stretching vibrations of C-NH-C were observed at 3450 cm^{-1} and
25
26 1126 cm^{-1} , respectively. The high-intensity peaks at 1628 cm^{-1} and 1405 cm^{-1}
27
28 corresponded to the asymmetric and symmetric stretching vibrations of the
29
30 carboxylate anions ($-\text{COO}^-$), respectively. Compared to the original CDs, the spectrum
31
32 of CDs-COOH showed the peak at around 3450 cm^{-1} was broadened and the sharp
33
34 peak at 1650 cm^{-1} was enhanced. These results indicate that plenty of carboxyl groups
35
36 were introduced after treatment of the CDs with NaOH and $\text{ClCH}_2\text{COONa}$.
37
38 Furthermore, as depicted in the spectrum of CDs-gIgG, the band at 3450 cm^{-1} became
39
40 wider, which was attributed to the increase of O-H and N-H stretching vibrations. The
41
42 typical bands associated with $-\text{CONH}-$ could be seen at around 1649 cm^{-1} and 1577
43
44 cm^{-1} , reflecting the conjugation of the antibody gIgG onto CDs-COOH.

45 46 47 48 **3.3. Principle of fluorescence immunosensor**

49
50 As depicted in Scheme 1, the as-prepared carboxyl-functionalized CDs were
51
52 used to label the gIgG antibody by virtue of the activated effect of EDC and NHS, the
53
54 resulting CDs-gIgG conjugate exhibited the same fluorescence properties as
55
56 CDs-COOH. In the presence of human IgG, the fluorescence intensity of this sensing
57
58 system obviously enhanced due to the specific interaction between gIgG and human
59
60 IgG. This antigen-induced fluorescence enhancement was either associated with the
surface polarity of antigen-antibody immunocomplex or the formation of a

1
2
3
4 immunocomplex coated layer, which further decreased the surface defects²⁷ of
5 CDs-COOH. Based on the above phenomena, we proposed a simple, rapid and direct
6 technique for quantitation of human IgG.
7
8

9 10 11 **3.4. Optimal conditions for human IgG detection**

12
13 The concentrations of CDs-gIgG have obvious impact on the immunoassay
14 performance. In order to obtain a wide linear range and high sensitivity, the effect of
15 CDs-gIgG dosage on the system was examined (Fig. 3A). The results show that the
16 fluorescence intensity enhanced with increasing concentration of CDs-gIgG. However,
17 the increasing tendency turned to a platform when the concentration of CDs-gIgG was
18 higher than 15 $\mu\text{g mL}^{-1}$. Therefore, 15 $\mu\text{g mL}^{-1}$ of CDs-gIgG was chosen in the further
19 experiments.
20
21

22 Since the immunocomplexes were stable in PBS, the antigen-antibody
23 immunoreactions were generally performed in this buffer.²⁸ Therefore, we chose 0.1
24 M PBS as the reaction medium. As seen from Fig. 3B, no significant changes of the
25 fluorescence intensity ratio $(F-F_0)/F_0$ were observed in solutions with pH between 5.0
26 and 9.0. Thus, in order to maintain antibody activity, the whole experimental
27 procedure was carried out at 37 °C for 30 min²⁹ in 0.1 M PBS of pH 7.4.
28
29

30 31 32 **3.5. Analytical performance**

33 We developed an immunosensing strategy based on CDs for human IgG
34 detection. Under the optimal conditions, the sensing performance of this system was
35 evaluated by adding various concentrations of human IgG into the CDs-gIgG. As
36 shown in Figure 4A, introduction of human IgG to CDs-gIgG produced a remarkable
37 fluorescence enhancement of the system without spectral shift. Furthermore, the
38 fluorescence intensities of CDs-gIgG increased monotonically with increasing
39 amounts of added human IgG. To quantify the human IgG, a calibration curve (Figure
40 4A, inset) was prepared by using a series of human IgG standard solutions at different
41 concentrations. As seen in Figure 4B, the curve showed a good linear relationship
42 between the fluorescence intensity ratio and human IgG concentrations in the range of
43
44
45
46
47
48
49
50
51
52
53
54
55
56
57
58
59
60

0.05-2.0 $\mu\text{g mL}^{-1}$, the corresponding analytical performance data could be seen in the first table of Table 3. The limit of detection (LOD) was comparable and even lower than those of many reported immunoassay methods for human IgG, such as chemiluminescence-based immunoassay,²⁹ fluorescence resonance energy transfer (FRET)-based immunoassay,^{30,31} flow-injection electrochemical immunoassay,³² time-resolved (TR) fluorescence immunoassay³³ and electrochemical immunoassay,^{34,35} and some of the results using various fluorescent labels were shown in the second table of Table 3. The obtained relative standard deviation (R.S.D.) was 2.11% for 0.1 $\mu\text{g mL}^{-1}$ of human IgG, demonstrating an excellent precision of the fluorescent probe.

3.6. Interference effect

The selectivity of the fluorescent probe was evaluated by testing the response of the fluorescent probe to multiple coexisting substances (such as amino acids, proteins and metal ions) under the optimal conditions in the case of 0.1 $\mu\text{g mL}^{-1}$ of human IgG (Fig. 5). The corresponding data is shown in Table 4. When the relative error (Er) exceeded $\pm 5\%$, each coexisting substance was regarded as an interfering agent. It was found that most ions and molecules at relatively high concentrations only caused negligible fluorescence change. However, when 10.0 $\mu\text{g mL}^{-1}$ of BSA was added to the CDs-gIgG solution, it exhibited a slight interference on the assay system. But when the concentration of BSA was down to 0.1 $\mu\text{g mL}^{-1}$, the relative error was still within tolerance limits ($< \pm 5\%$). The results confirmed the excellent selectivity of this fluorescent probe to human IgG detection.

3.7. Real sample application

In order to estimate the application potential of this fluorescent probe, the levels of human IgG in seven normal human sera were evaluated with this method. Prior to the assay, the serum samples were diluted appropriately to ensure the concentrations of human IgG in the linear range. As shown in Table 5, the concentrations of human IgG in seven human serum samples were found from 8.5 mg mL^{-1} to 14.3 mg mL^{-1} ,

1
2
3
4 which was in the range of the clinical reference³⁶ and consistent with that (from 9.1
5 mg mL⁻¹ to 13.3 mg mL⁻¹) in the literature.³⁷ Known amount of human IgG standard
6 solution was spiked into the diluted samples to perform the recovery tests. The
7 recoveries for the spiked human IgG were between 95.8% and 111.5%, and the
8 relative standard deviations were all less than 2.0%, indicating the feasibility of
9 proposed method.
10
11
12
13
14
15
16
17

18 **4. Conclusion**

19
20 In summary, CDs with a quantum yield as high as ca. 74.6% were synthesized
21 and carboxylated to introduce plenty of carboxyl groups. Then, carboxylated CDs
22 were attached to antibody gIgG to form the CDs-labeled gIgG conjugate. A
23 fluorescence immunoassay strategy was constructed with the addition of model
24 analyte human IgG to CDs-gIgG, which enables the quantitative measurements of the
25 human IgG. The results indicate that the proposed method has excellent performance
26 for the detection of human IgG with a wide linear range and low detection limit.
27 Moreover, the concentrations of IgG in human sera have been determined with
28 satisfactory results. It is expected that the easy and direct strategy would promote the
29 application of CDs-based sensor in fluorescence immunoassay methods and open new
30 opportunities for development of the immunofluorescence technique.
31
32
33
34
35
36
37
38
39
40
41
42

43 **Acknowledgements**

44
45 This work was supported by the National Natural Science Foundation of China
46 (No. 5151072074).
47
48
49

50 **References**

- 51
52
53 1 M. C. Zhang, Q. E. Wang and H. S. Zhuang, *Anal. Bioanal. Chem.*, 2006, **386**,
54 1401.
55
56 2 S. C. Zhu, Q. Zhang and L. H. Guo, *Anal. Chim. Acta*, 2008, **624**, 141.
57
58 3 A. R. M. Bustos, L. T. Alfonso, J. R. Encinar, J. M. C. Fernández, R. Pereiro and
59 A. S. Medel, *Biosensors and Bioelectronics*, 2012, **33**, 165.
60

- 1
2
3
4 Y. D. Zhu, J. Peng, L. P. Jiang and J. J. Zhua, *Analyst*, 2014, **139**, 649.
5
6 P. S. Petrou, S. Georgiou, I. Christofidis and S. E. Kakabakos, *J. Immunol. Methods*,
7
8 2002, **266**, 175.
9
10 Z. Y. Fan, Y. S. Keum, Q. X. Li, W. L. Shelver and L. H. Guo, *J. Environ. Monit.*,
11
12 2012, **14**, 1345.
13
14 J. Shen, L. D. Sun and C. H. Yan, *Dalton Trans.*, 2008, **42**, 5687.
15
16 A. R. Clapp, I. L. Medintz, J. M. Mauro, B. R. Fisher, M. G. Bawendi and H. J.
17
18 Mattoussi, *J. Am. Chem. Soc.*, 2004, **126**, 301.
19
20 T. Jamieson, R. Bakhshi, D. Petrova, R. Pocock, M. Imani and A. M. Seifalian,
21
22 *Biomaterials*, 2007, **28**, 4717.
23
24 U. R. Genger, M. Grabolle, S. C. Jaricot, R. Nitschke and T. Nann, *Nature*
25
26 *methods*, 2008, **5**, 763.
27
28 S. N. Baker and G. A. Baker, *Angew. Chem. Int. Ed.*, 2010, **49**, 6726.
29
30 X.Y. Xu, R. Ray, Y. L. Gu, H. J. Ploehn, L. Gearheart, K. Raker and W. A.
31
32 Scrivens, *J. Am. Chem. Soc.*, 2004, **126**, 12736.
33
34 S. C. Ray, A. Saha, N. R. Jana and R. Sarkar, *J. Phys. Chem. C*, 2009, **113**, 18546.
35
36 H. T. Li, X. D. He, Y. Liu, H. Huang, S. Y. Lian, S. T. Lee and Z. H. Kang,
37
38 *Carbon*, 2011, **49**, 605.
39
40 S. J. Zhu, Q. N. Meng, L. Wang, J. H. Zhang, Y. B. Song, H. Jin, K. Zhang, H. C.
41
42 Sun, H. Y. Wang and B. Yang, *Angew. Chem. Int. Ed.*, 2013, **52**, 3953.
43
44 B. D. Yin, J. H. Deng, X. Peng, Q. Long, J. N. Zhao, Q. J. Liu, Q. Chen, H. T. Li,
45
46 H. Tang, Y. Y. Zhang and S. Z. Yao, *Analyst*, 2013, **138**, 6551.
47
48 A. S. Krishna, C. Radhakumary and K. Sreenivasan, *Analyst*, 2013, **138**, 7107.
49
50 H. L. Li, Y. W. Zhang, L. Wang, J. Q. Tian and X. P. Sun, *Chem. Commun.*, 2011,
51
52 **47**, 961.
53
54 J. H. Liu, J. S. Li, Y. Jiang, S. Yang, W. H. Tan and R. H. Yang, *Chem. Commun.*,
55
56 2011, **47**, 11321.
57
58 B. L. Xu, C. Q. Zhao, W. L. Wei, J. S. Ren, D. Miyoshi, N. Sugimoto and X. G.
59
60 Qu, *Analyst*, 2012, **137**, 5483.
21 P. G. Luo, S. Sahu, S. T. Yang, S. K. Sonkar, J. P. Wang, H. F. Wang, G. E. LeCroy,

- 1
2
3
4 L. Cao and Y. P. Sun, *J. Mater. Chem. B*, 2013, **1**, 2116.
5
6 22 L. Cao, X. Wang, M. J. Mezirani, F. S. Lu, H. F. Wang, P. G. Luo, Y. Lin, B. A.
7 Harruff, L. M. Veca, D. Murray, S. Y. Xie and Y. P. Sun, *J. Am. Chem. Soc.*, 2007,
8 **129**, 11318.
9
10 23 L. M. Zhang, J. G. Xia, Q. H. Zhao, L. W. Liu and Z. J. Zhang, *small*, 2010, **6**,
11 537.
12
13 24 B. F. Han, W. X. Wang, H. Y. Wu, F. Fang, N. Z. Wang, X. J. Zhang and S. K. Xu,
14 *Colloids and Surfaces B: Biointerfaces*, 2012, **100**, 209.
15
16 25 H. Zhu, X. L. Wang, Y. L. Li, Z. J. Wang, F. Yang and X. R. Yang, *Chem.*
17 *Commun.*, 2009, 5118.
18
19 26 T.J. Burke, K.R. Loniello, J.A. Beebe and K.M. Ervin, *Combinatorial Chemistry*
20 *& High Throughput Screening*, 2003, **6**, 183.
21
22 27 M. Idowu, E. Lamprecht and T. Nyokong, *J. Photochem. Photobiol. A*, 2008, **198**,
23 7.
24
25 28 S. Bi, Y. M. Yan, X. Y. Yang and S. S. Zhang, *Chem. Eur. J.*, 2009, **15**, 4704.
26
27 29 G. X. Qin, S. L. Zhao, Y. Huang, J. Jiang and F. G. Ye, *Anal. Chem.*, 2012, **84**,
28 2708.
29
30 30 M. Wang, W. Hou, C. C. Mi, W. X. Wang, Z. R. Xu, H. H. Teng, C. B. Mao and S.
31 K. Xu, *Anal. Chem.*, 2009, **81**, 8783.
32
33 31 J. Wang, T. Liu, Y. Cao, X. Hua, H. Wang, H. Zhang, X. Li and Y. Zhao, *Colloids*
34 *Surf., A*, 2007, **302**, 168.
35
36 32 D. Tang, R. Niessner and D. Knopp, *Biosensors and Bioelectronics*, 2009, **24**,
37 2125.
38
39 33 C. G. Niu, J. Liu, P. Z. Qin, G. M. Zeng, M. Ruan and H. He, *Anal. Biochem.*,
40 2011, **409**, 244.
41
42 34 H. Zarei, H. Ghourchian, K. Eskandari and M. Zeinali, *Anal. Biochem.*, 2012, **421**,
43 446.
44
45 35 Z. Y. Zhong, M. X. Li, D. B. Xiang, N. Dai, Y. Qing, D. Wang and D. P. Tang,
46 *Biosensors and Bioelectronics*, 2009, **24**, 2246.
47
48
49
50
51
52
53
54
55
56
57
58
59
60 36 T. Fonong and G. A. Rechnitz, *Anal. Chem.*, 1984, **56**, 2586.

1
2
3
4 37 Z. X. Wang, H. F. Gao and Z. F. Fu, *Analyst*, 2013, **138**, 6753.
5
6
7

8 **Figure Captions**

9
10 **Scheme 1.** Schematic illustration for the detection mechanism of human IgG
11 using the carboxyl group-functionalized carbon dots.
12

13
14 **Fig. 1** (A) Fluorescence emission spectra (with progressively longer excitation
15 wavelengths from 340 nm to 480 nm) of CDs (A); (B) Fluorescence emission spectra
16 (with progressively longer excitation wavelengths from 300 nm to 400 nm) of CDs
17 (B). The emission spectral intensities are normalized in the inset of (A) and (B); (C)
18 UV-Vis absorption spectra of gIgG (Abs, black dot), CDs-COOH (Abs, blue solid)
19 and CDs-gIgG (Abs, red dash). Insets: photographs of the CDs-COOH (a) and
20 CDs-gIgG (b) aqueous solution taken under 365 nm UV light; (D) Fluorescence
21 excitation and emission spectra of CDs-COOH and CDs-gIgG.
22
23

24
25
26
27
28
29 **Fig. 2** FT-IR spectra of CDs, CDs-COOH and CDs-gIgG.
30

31
32 **Fig. 3** (A) Effect of the concentration of CDs-gIgG on the fluorescence change
33 $(F-F_0)/F_0$ of the system (Conditions: 1-25 $\mu\text{g mL}^{-1}$ CDs-gIgG, 0.1 $\mu\text{g mL}^{-1}$ human IgG,
34 at 37 °C for 30 min); (B) Effect of pH value on the $(F-F_0)/F_0$ of the system
35 (Conditions: 15 $\mu\text{g mL}^{-1}$ CDs-gIgG, 0.1 $\mu\text{g mL}^{-1}$ human IgG, pH 5-9, at 37 °C for 30
36 min).
37
38

39
40
41
42 **Fig. 4** (A) Fluorescence emission spectra of CDs-gIgG-human IgG. Human IgG
43 concentrations: 0-20 $\mu\text{g mL}^{-1}$. Buffer solution: 0.1 M PBS buffer (pH 7.4). Inset is a
44 calibration curve of the $(F-F_0)/F_0$ against the concentration of human IgG; (B) A linear
45 region in the range of 0.05 $\mu\text{g mL}^{-1}$ to 2.0 $\mu\text{g mL}^{-1}$.
46
47

48
49
50
51 **Fig. 5** Selectivity of the CDs-gIgG fluorescent probe to 0.1 $\mu\text{g mL}^{-1}$ human IgG
52 over the coexisting substances under the optimal conditions.
53
54

55 **Table Captions**

56
57 **Table 1.** Quantum yield of CDs, CDs-COOH and CDs-gIgG
58

59 **Table 2.** Comparing fluorescence polarization values (P) of CDs-COOH with
60

CDs-gIgG

Table 3. The characteristic performance data for the determination of human IgG using CDs as a fluorescent label

Table 4. Fluorescence change responses of the system to diverse coexisting substances

Table 5. Recovery tests of human IgG spiked in the human serum samples

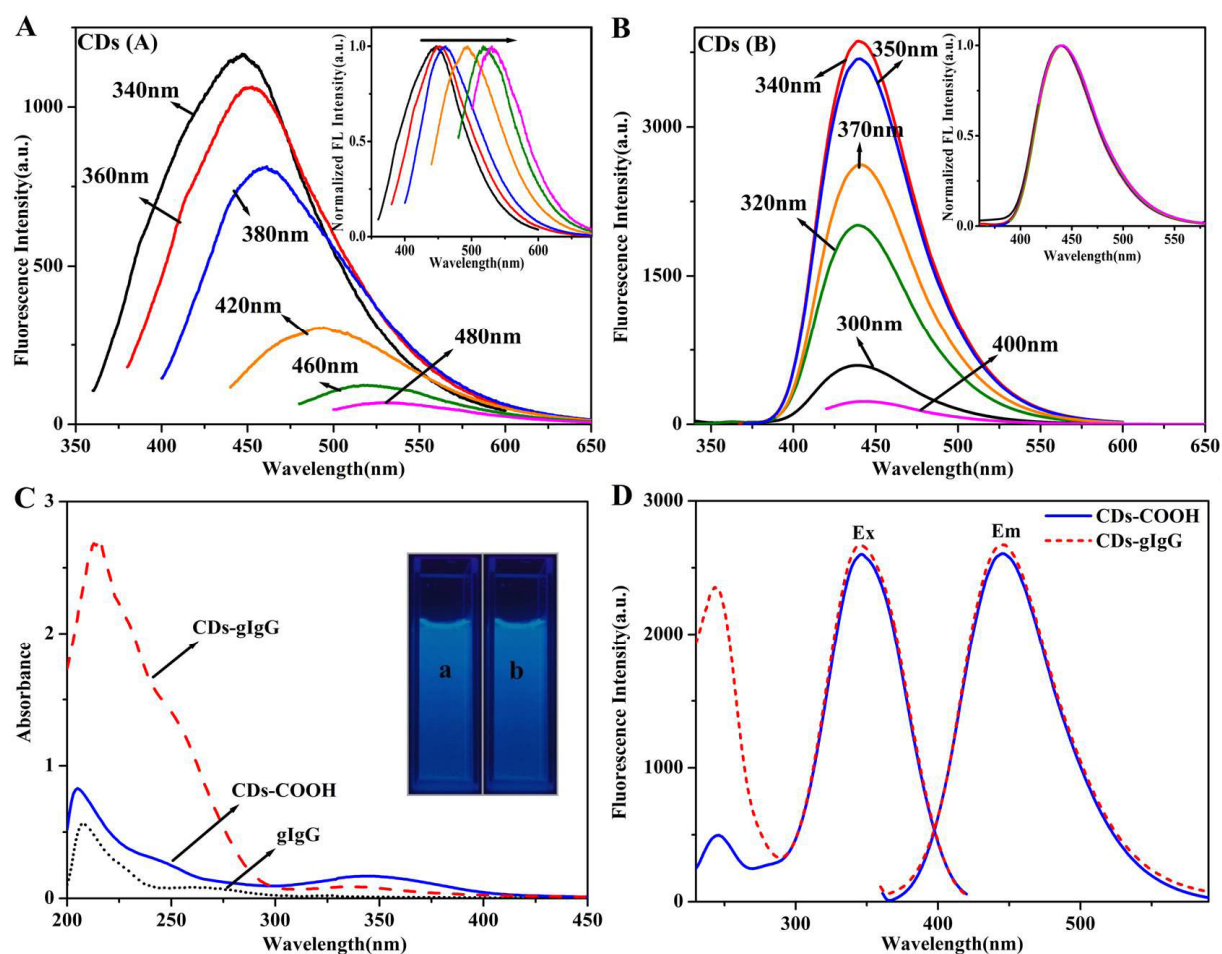


Fig. 1

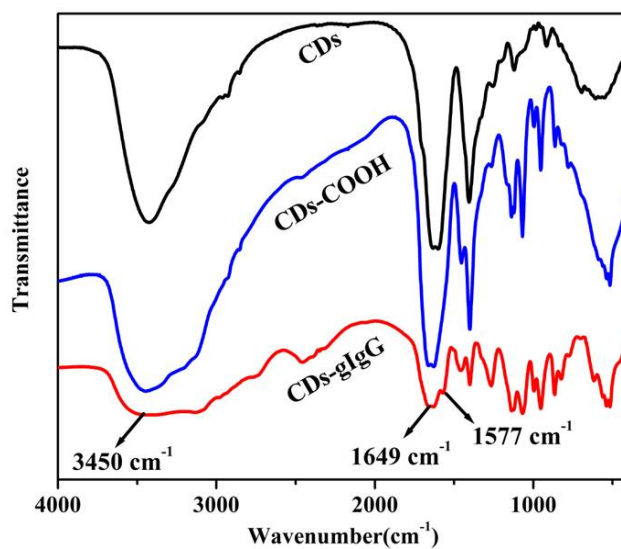
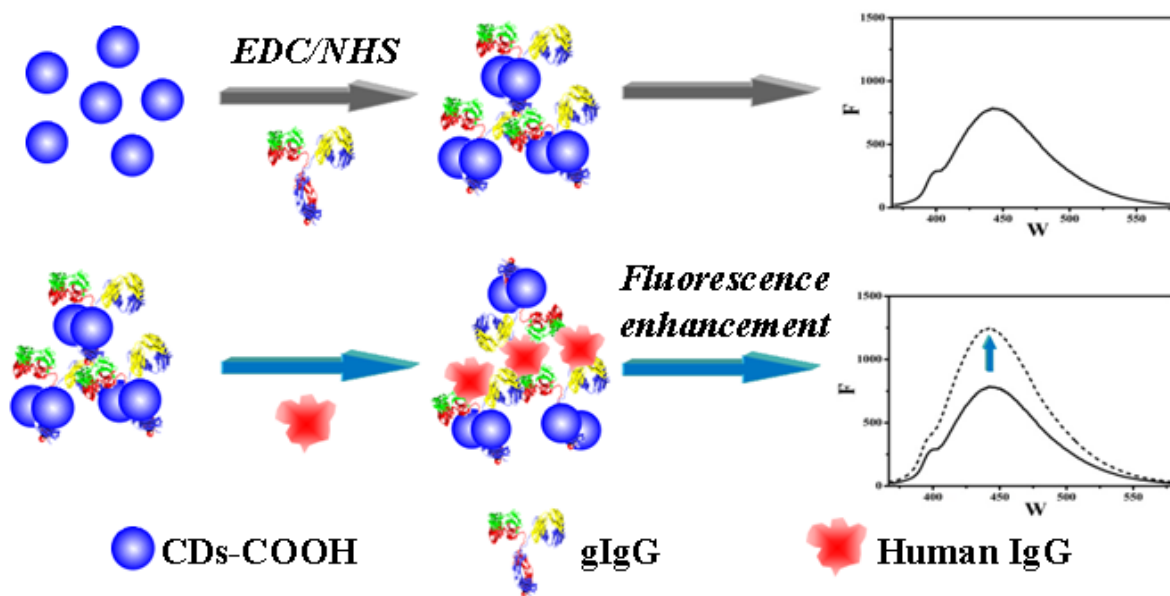


Fig. 2



Scheme 1

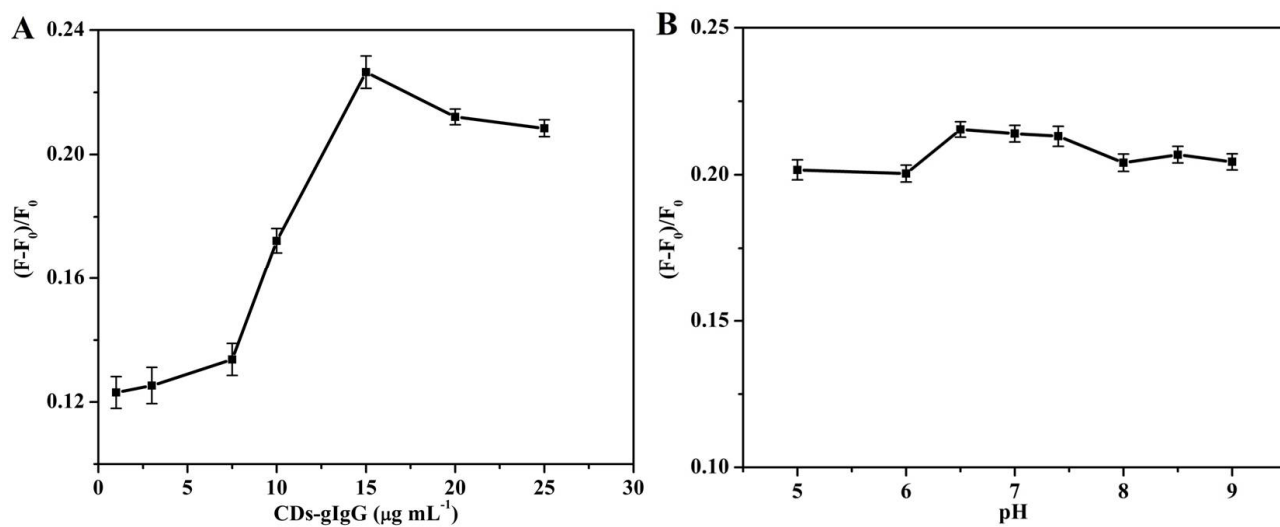


Fig. 3

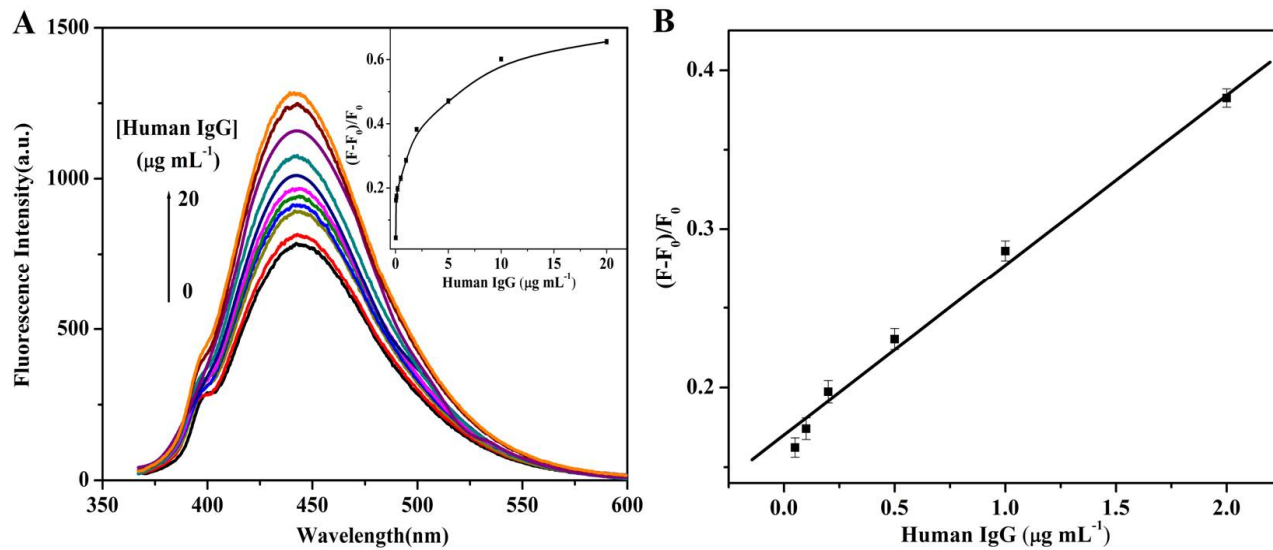


Fig. 4

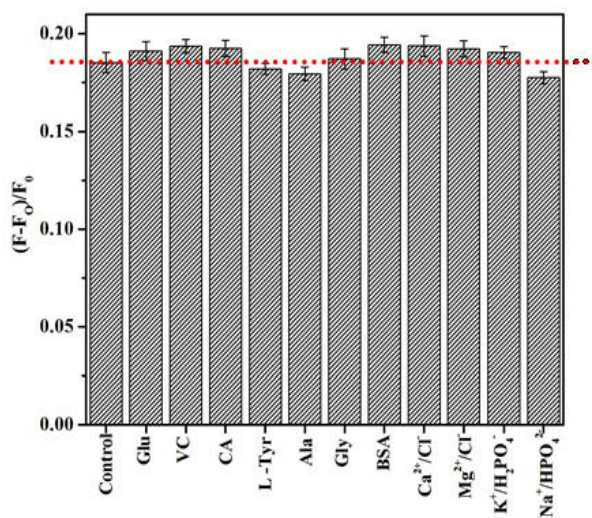


Fig. 5

Table 1 Quantum yield of CDs, CDs-COOH and CDs-gIgG

Sample	Integrated emission intensity (I)	Abs. at 360 nm (A)	Refractive index of solvent (η)	Quantum Yield (Φ)
Quinine sulfate	214083.0	0.036	1.33	0.54
CDs (A)	13218.5	0.018	1.33	0.067
CDs (B)	188952.5	0.023	1.33	0.746
CDs (B)-COOH	26921.2	0.034	1.33	0.072
CDs-gIgG	35469.1	0.044	1.33	0.073

CDs (A) and CDs (B) are prepared through hydrothermal treatment of citric acid in the absence and presence of ethylenediamine, respectively. The conjugate CDs-gIgG is formed using CDs (B)-COOH as a fluorescent label.

Table 2 Comparing fluorescence polarization values (P) of CDs-COOH with CDs-gIgG

	i_{\perp}	i_{\parallel}	I_{\perp}	I_{\parallel}	G (i_{\perp}/i_{\parallel})	P	*mP
CDs-COOH	675	500	732	1050	1.35	0.030	30
CDs-gIgG	700	521	760	1122	1.34	0.048	48

i_{\parallel} , I_{\parallel} and i_{\perp} , I_{\perp} represent the horizontally and vertically polarized emission intensities, respectively, and G is a correction factor. *1 P=10³ mP.

Table 3 The characteristic performance data for the determination of human IgG using CDs as a fluorescent label

Parameters	Results
Linear calibration range	0.05-2.0 $\mu\text{g mL}^{-1}$
Regression equation	$(F-F_0)/F_0=0.1102*C (\mu\text{g mL}^{-1}) + 0.1681$
Correlation coefficient	$R^2 = 0.9898$
Detection limit(*3S _b /slope)	0.01 $\mu\text{g mL}^{-1}$
R.S.D (%)	2.11% (n=11)

Comparison of reported immunoassay for human IgG using various fluorescent labels

Fluorescent labels	Immunoassay methods	Detection limit ($\mu\text{g mL}^{-1}$)	Ref.
Organic dyes	Chemiluminescence	0.005	29
NaYF ₄ :Yb, Er	FRET	0.88	30
QDs	FRET	0.02	31
Rare earths chelate	TR fluorescence	0.005	33

*C is the sample concentration. *S_b is standard deviation of the blank samples

Table 4 Fluorescence change responses of the system to diverse coexisting substances

Coexisting substances	Concentration	Relative error (%)
Glucose	1.5 $\mu\text{g mL}^{-1}$	3.2
L-(+) Ascorbic acid	1.5 $\mu\text{g mL}^{-1}$	4.6
Citric acid	1.5 $\mu\text{g mL}^{-1}$	3.9
L-Tyrosine	1.5 $\mu\text{g mL}^{-1}$	-1.7
Lactamic acid	1.5 $\mu\text{g mL}^{-1}$	-3.1
Glycine	1.5 $\mu\text{g mL}^{-1}$	1.0
BSA	0.1 $\mu\text{g mL}^{-1}$	4.9
Ca ²⁺ , Cl ⁻	2.0 $\mu\text{g mL}^{-1}$	4.6
Mg ²⁺ , Cl ⁻	2.0 $\mu\text{g mL}^{-1}$	3.8
K ⁺ , H ₂ PO ₄ ⁻	2.0 $\mu\text{g mL}^{-1}$	2.8
Na ⁺ , HPO ₄ ²⁻	2.0 $\mu\text{g mL}^{-1}$	-4.1

Table 5 Recovery tests of human IgG spiked in the human serum samples

Sample number	Found in		Total found ($\mu\text{g mL}^{-1}$)	R.S.D. (%; n=3)	Recovery (%)	Found in original sample (mg mL^{-1})
	diluted sample ($\mu\text{g mL}^{-1}$)	Added ($\mu\text{g mL}^{-1}$)				
1	0.34	0.1	0.441	1.09	101.2	8.5
2	0.52	0.1	0.618	1.47	98.3	13.0
3	0.45	0.1	0.55	0.90	104.6	11.3
4	0.38	0.1	0.476	0.89	95.8	9.5
5	0.54	0.1	0.65	1.92	111.5	13.4
6	0.43	0.1	0.531	1.01	101	10.7
7	0.57	0.1	0.679	1.09	109.2	14.3